Neurobiology of Aging 97 (2021) 56–64

Contents lists available at ScienceDirect

Neurobiology of Aging

journal homepage: www.elsevier.com/locate/neuaging

Increased isoform-specific phosphodiesterase 4D expression is associated with pathology and cognitive impairment in Alzheimer's disease

Dean Paes[a,b], Roy Lardenoije[a,c,d], Riccardo M. Carollo[a], Janou A.Y. Roubroeks[a,e], Melissa Schepers[a,b], Paul Coleman[f,g], Diego Mastroeni[a,f,g], Elaine Delvaux[f,g], Ehsan Pishva[a,e], Katie Lunnon[e], Tim Vanmierlo[a,b], Daniel van den Hove[a,h], Jos Prickaerts[a,*]

[a] Department of Psychiatry & Neuropsychology, School for Mental Health and Neuroscience, Maastricht University, Maastricht, the Netherlands
[b] Department of Neuroimmunology, Biomedical Research Institute, Hasselt University, Diepenbeek, Belgium
[c] Department of Psychiatry and Psychotherapy, Universitätsmedizin Göttingen, Georg-August-Universität, Göttingen, Germany
[d] Department of Psychiatry, McLean Hospital, Harvard Medical School, Belmont, MA, USA
[e] Institute of Biomedical and Clinical Sciences, University of Exeter Medical School, University of Exeter, Exeter, UK
[f] L.J. Roberts Center for Alzheimer's Research, Banner Sun Health Research Institute, Sun City, AZ, USA
[g] Biodesign Institute, Neurodegenerative Disease Research Center, Arizona State University, Tempe, AZ, USA
[h] Department of Psychiatry, Psychosomatics and Psychotherapy, University of Würzburg, Würzburg, Germany

ARTICLE INFO

Article history:
Received 9 April 2020
Received in revised form 16 September 2020
Accepted 4 October 2020
Available online 9 October 2020

Keywords:
Alzheimer's disease
Phosphodiesterase 4D (PDE4D)
Transcript variants
DNA methylation
Braak stage
Cognitive impairment

ABSTRACT

Pharmacological phosphodiesterase 4D (PDE4D) inhibition shows therapeutic potential to restore memory function in Alzheimer's disease (AD), but will likely evoke adverse side effects. As *PDE4D* encodes multiple isoforms, targeting specific isoforms may improve treatment efficacy and safety. Here, we investigated whether PDE4D isoform expression and *PDE4D* DNA methylation is affected in AD and whether expression changes are associated with severity of pathology and cognitive impairment. In post-mortem temporal lobe brain material from AD patients ($n = 42$) and age-matched controls ($n = 40$), we measured PDE4D isoform expression and *PDE4D* DNA (hydroxy)methylation using quantitative polymerase chain reaction and Illumina 450k Beadarrays, respectively. Linear regression revealed increased PDE4D1, -D3, -D5, and -D8 expression in AD with concurrent (hydroxy)methylation changes in associated promoter regions. Moreover, increased PDE4D1 and -D3 expression was associated with higher plaque and tau pathology levels, higher Braak stages, and progressed cognitive impairment. Future studies should indicate functional roles of specific PDE4D isoforms and the efficacy and safety of their selective inhibition to restore memory function in AD.

1. Introduction

Impaired memory function in Alzheimer's disease (AD) patients has a debilitating effect on daily activities and, consequently, negatively affects the quality of life of patients, their caretakers, and family (Schneider et al., 1999). The second messenger cyclic adenosine monophosphate (cAMP) is crucial in the molecular signaling cascades underlying memory function (Kandel, 2012). Intracellular cAMP levels are mainly controlled through degradation by the phosphodiesterase 4 (PDE4) enzyme family (Houslay, 2010). Accordingly, previous studies have shown that PDE4 inhibition can improve memory consolidation processes in rodents (Vanmierlo et al., 2016). In humans, the PDE4 inhibitor roflumilast was found to enhance verbal learning in young adults and old healthy volunteers (Blokland et al., 2019; Van Duinen et al., 2018). Thus, PDE4 inhibition seems to hold clinical potential as a treatment to enhance memory functioning. The therapeutic potential in AD is supported by the finding that PDE4 inhibition can restore memory impairments induced by intra-hippocampal injections with amyloid-β in rats (Cheng et al., 2010). Moreover, in a mouse model of tauopathy, the number of tau aggregates was reduced after administration of the nonselective PDE4 inhibitor rolipram (Myeku et al., 2016). Despite these promising results, progression of new PDE4

Tim Vanmierlo, Daniel van den Hove, and Jos Prickaerts contributed equally to this work.

* Corresponding author at: Department of Psychiatry & Neuropsychology, School for Mental Health and Neuroscience, Maastricht University, PO Box 616, 6200 MD, Maastricht, the Netherlands. Tel.: +31 43 3881168; fax: +31 43 3671096.
E-mail address: jos.prickaerts@maastrichtuniversity.nl (J. Prickaerts).

https://doi.org/10.1016/j.neurobiolaging.2020.10.004

inhibitors into the clinic is hampered by the occurrence of dose-limiting side effects, mainly nausea and emesis. More selective inhibition of PDE4 subtypes or isoforms may circumvent these adverse effects. In the present study, we investigated whether expression regulation of PDE4D isoforms is altered in AD brain material to identify potential targets for more selective PDE4 inhibition. The PDE4 family consists of 4 genes (PDE4A-D) of which *PDE4D* seems to be mostly involved in the modulation of cognitive functions (Zhang et al., 2017). Hence, inhibitors selective for PDE4D have been developed to investigate their cognition-enhancing potential. These new selective PDE4D inhibitors have been found to enhance memory performance in rodents, including models of AD (Ricciarelli et al., 2017; Zhang et al., 2018). The procognitive effects of PDE4D-specific inhibition are supported by *PDE4D* knock-down studies (Baumgartel et al., 2018). The memory-enhancing potential of PDE4D inhibition has also been tested in Phase I clinical trials (ClinicalTrials.gov Identifier: NCT02648672 and NCT02840279) and currently, preparations are under way to initiate a Phase II trial in patients with early-stage AD (ClinicalTrials.gov Identifier: NCT03817684). Notably, PDE4D inhibition is also hypothesized to induce emetic side effects given its expression in brain areas involved in emesis, that is, the area postrema, and based on gene deletion studies (Mori et al., 2010; Robichaud et al., 2002). The human *PDE4D* gene gives rise to multiple protein isoforms, that is, PDE4D1-9, through alternative promoters and alternative splicing. These isoforms regulate a multitude of different processes and are localized to specific compartments within the cell owing to specific amino acids in the N-terminal domain (Houslay, 2010; Houslay et al., 2007). Hence, by inhibiting specific PDE4D isoforms, it can be argued that memory-enhancing effects could be retained without evoking side effects (Schepers et al., 2019). Despite the potential of PDE4D isoform-specific inhibition as a safe and efficacious treatment strategy in AD, the role of PDE4D isoforms in the context of specific brain functions or AD has only sporadically been described (McLachlan et al., 2007; Perez-Torres et al., 2000; Ugarte et al., 2015).

PDE4D isoforms showing high or increased expression in AD could be interesting targets, as these isoforms may contribute largely to cAMP hydrolysis and consequently impede memory functioning. PDE4D isoform expression is likely controlled by epigenetic mechanisms to regulate, for example, isoform-specific promoter accessibility. Previous research indicated that epigenetic modifications at the histone level influence promoter accessibility in the *PDE4D* gene and consequently affect isoform-specific expression in vascular smooth muscle cells (Tilley and Maurice, 2005). At the nucleotide level, epigenetic processes can reversibly influence transcription through conversion of unmethylated cytosines (UC) into methylated (5mC) or hydroxymethylated (5hmC) cytosines. Specific changes in DNA methylation and hydroxymethylation have previously been associated with AD (Smith et al., 2019). Recently, *PDE4D* was found those genes displaying differentially methylated in AD in an epigenome-wide association study (Lardenoije et al., 2019).

To investigate whether PDE4D isoform expression is altered in AD and whether this is associated with epigenetic changes at specific positions in the *PDE4D* gene, we established PDE4D expression and epigenetic profiles of human post-mortem brain material of AD patients and age-matched controls. Since AD is a progressive disease, we also explored whether changes in expression were associated with region-specific plaque and tau load, Braak stage, and the degree of cognitive impairment.

2. Methods

2.1. Brain material and study cohort

Informed consent was obtained from all individual participants included in the study. Human post-mortem brain material from the middle temporal gyrus (MTG) of AD patients and neurologically healthy controls was obtained from the Banner Sun Health Research Institute in Sun City, AZ. For every sample information on Mini-Mental State Examination (MMSE) score (Folstein et al., 1975), gender, age, post-mortem interval (PMI), *APOE* ε4 possession, amyloid-β plaque load, tau tangle load, Braak stage, and diagnosis were documented and tissue was prepared by standardized procedures (Beach et al., 2015). Braak staging was evaluated as previously described (Braak and Braak, 1991). AD diagnostic criteria followed guidelines for the National Institute on Aging-Reagan Institute criteria (Consensus Recommendations for the Postmortem Diagnosis of Alzheimer's Disease, 1997) combined with clinical diagnosis reports. Samples collected after a PMI of more than 5 hours and samples from patients with comorbidities were excluded. A total of 82 samples were included from AD patients ($n = 42$) and age- and gender-matched neurologically healthy controls ($n = 40$) with an average PMI of 2.8 hours. For subsequent analysis investigating associations between expression and MMSE score, cases for which cognitive performance in the MMSE was assessed longer than 36 months before death were excluded, leaving a subset of 41 cases. A detailed description of the cohort demographics can be found in Table 1.

2.2. RNA isolation, complementary DNA synthesis, and qPCR

Total RNA was isolated from frozen MTG tissue using the TRIzol Plus RNA Purification Kit (Life Technologies, Carlsbad, CA) following the manufacturer's protocol. Isolated RNA pellets were dissolved in RNAse-free water and assessed for quantity and quality (average RIN: 9.1) using a Nanodrop ND-1000 spectrophotometer (Thermo Scientific, DE) and Bioanalyzer (Agilent). Then, complementary DNA was synthesized using the Revert Aid First Strand Synthesis Kit (Thermo Scientific, Landsmeer, Netherlands) according to the manufacturer's protocol.

TaqMan-based quantitative polymerase chain reaction (qPCR) primers were used for the following PDE4D isoforms: PDE4D2, PDE4D4, PDE4D5, PDE4D6, PDE4D8, and PDE4D9 (Applied Biosystems, Foster City, CA, USA). PDE4D2 could not be detected. Primers were designed for PDE4D1, PDE4D3, and PDE4D7 as no TaqMan-based qPCR primers were available for these isoforms (SIGMA Life Science). Housekeeping gene expression of *EIF4A2* and *TOP1* showed the most stable expression based on geNorm criteria and was used for normalization (Vandesompele et al., 2002). TaqMan probe and primer sequences are listed in Table 2. TaqMan-based qPCR was performed using TaqMan Assay 20x and TaqMan Universal Master Mix II, with UNG 2x (Applied Biosystems) following the manufacturer's protocol. For qPCR using primers, SensiMix 2X (Bioline) was used according to the manufacturer's protocol. All reactions were performed using 6 ng complementary DNA on a LightCycler 480 (Roche).

2.3. Tissue preparation for (hydroxy)methylomic profiling

DNA was isolated from the MTG at the Banner Sun Health Research Institute. From 81 of the 82 subjects, a total of 76 mg of

Table 1
Demographic characteristics of the cohort

Characteristic	Non-demented controls	AD patients
Gender (male/female)	20/20	19/23
APOE ε4 (present/absent)	9/31	27/15
Braak stage (I-II/III-IV/V-VI)	16/24/0	0/14/28
Age, mean (SD)	84.3 (5.81)	85.1 (6.49)
PMI, mean (SD)	2.77 (0.75)	2.75 (0.73)

Key: AD, Alzheimer's disease; PMI, post-mortem interval; SD, standard deviation.

Table 2
TaqMan probe and primer sequences

Isoform	Forward primer (5′-3′)	Reverse primer (5′-3′)
PDE4D1	AGAACTGAGTCCCCCTTTCC	TGAGCTCCCGATTAAGCATC
PDE4D3	CCACGATAGCTGCTCAAACA	GTGCCATTGTCCACATCAAA
PDE4D7	GAACATTCAACGACCAACCA	TTCCGGGACATAGACTTTGG
EIF4A2	GGTCAGGGTCAAGTCGTGTT	CCCCTCTGCCAATTCTGTGA
TOP1	CCCTGTACTTCATCGACAAGC	CCACAGTGTCCGCTGTTTC
Isoform	**TaqMan probe sequence (5′-3′)**	**TaqMan Assay ID**
PDE4D2	TCCGAGCATGGCGGGAGGAGGCCTA	Rn01494075_g1
PDE4D4	TTCCAGGGACTCAGGCGTTTTGATG	Hs01588302_m1
PDE4D5	CACATACATGTTTTGATGTGGACAA	Hs01588303_m1
PDE4D6	ATAAAGTTTAAAAGGATGCTTAATC	Hs01572151_m1
PDE4D8	GTTTCTCAAAGTCCTACAGTTTTGA	Hs00938323_m1
PDE4D9	GCAGTTTGTTTTGATGTGGACAATG	Hs01572149_m1

frozen tissue was obtained (Beach et al., 2015). Tissue was digested at 55 °C in lysis buffer (100 mM Tris-HCl pH 8.5, 200 mM NaCl, 5 mM ethylenediaminetetraacetic acid, 100 μg/mL Proteinase K [Sigma-Aldrich, St. Louis, MO], and 0.2% sodium dodecyl sulfate) and homogenized in a pellet mixer (Kontes). After addition of RNase (Qiagen, Valencia, CA, USA), DNA was isolated by means of phenol/chloroform (Sigma) extraction followed by ethanol precipitation and resuspension in TE buffer (pH 8.0). Ultimately, DNA samples were quantified and checked for purity by means of spectrophotometry.

2.4. Oxidative bisulfite conversion and DNA (hydroxy)methylation assay

The (oxidative) bisulfite (oxBS) conversion procedures and HumanMethylation450 BeadChip array were carried out at ServiceXS (ServiceXS B.V., Leiden, the Netherlands), in accordance to the manufacturer' protocols and as described previously (Lardenoije et al., 2019). Briefly, a TrueMethylTM 24 kit version 2.0 by CEGXTM (Cambridge Epigenetix Limited, Cambridge, UK) was used to convert the isolated genomic DNA (gDNA) by bisulfite (BS) or oxBS treatments to detect and localize 5mC and 5hmC marks at single-base resolution. Before conversion, gDNA quality was assessed using a PicoGreen assay (Invitrogen, Carlsbad, CA, USA) and high molecular weight gDNA was quantified by gel-electrophoresis. Upon purification and denaturation, high molecular weight gDNA (0.5 μg per treatment) was used for DNA oxidation or mock DNA oxidation treatments followed by BS conversion. DNA yield was assessed by Qubit ssDNA assay (Invitrogen) and qualitative assessment of 5hmC oxidation and BS conversion was performed using a restriction quality control. Then, 8 μL of each DNA sample was used for amplification and hybridization on the HumanMethylation450 BeadChip (Illumina, Inc., San Diego, CA, USA) according to the Illumina "Infinium II Methylation Assay Manual" protocol. Eventually, the Illumina iScan was used to scan the samples.

2.5. Processing of DNA (hydroxy)methylation assay data

For (hydroxy)methylomic profiling, data were processed and analyzed using R statistical programming language (version 3.5.3) (R Development Core Team, 2019) and RStudio (version 1.2.1335) (RStudio Team, 2019). The minfi package (version 1.28.4) was used to load raw IDAT files from the Illumina iScan (Aryee et al., 2014). Probes that cross-hybridize, locate to X and Y chromosomes and probes binding within 10 bp of a common SNP location were removed (Chen et al., 2013). Remaining probes were filtered using the "pfilter" function of the wateRmelon package (version 1.26.0) (6414 probes were removed) (Pidsley et al., 2013). Data from 397,160 remaining probes were split into 2 sets of beta values according to the oxBS and BS arrays, representing 5mC and 5mC + 5hmC, respectively. These data were *dasen* normalized using the wateRmelon package (Pidsley et al., 2013). The maximum likelihood methylation levels (MLML) method was used, by means of the "MLML" function within the MLML2R package (version 0.3.2), to calculate the proportions of 5mC, 5hmC, and UC by combining the signal from the BS and oxBS arrays as input (Kiihl et al., 2019; Qu et al., 2013). Subsequently, probes showing either a 5hmC value of zero in at least half of the cases or BS beta value lower than 0.1 were filtered out (112,697 5hmC values were excluded). Data distributions of raw and normalized beta values per sample were visualized in boxplots and density plots to identify outliers (3 samples were excluded due to clear deviation from the other samples; data not shown). Data were processed again upon removal of these outliers.

After data processing, 78 samples remained, with 397,160 remaining probes for 5mC and UC, and 284,463 5hmC probes. Data were split into 2 sets of beta values according to the oxBS and BS arrays, representing 5mC and 5mC + 5hmC, respectively.

2.6. Statistical analysis

Raw expression data from the LightCycler 480 were analyzed using LinRegPCR to determine logarithmic fluorescence values at cycle zero (Ruijter et al., 2009). qPCR reactions that did not show fluorescent signal amplification were excluded from further analysis. Logarithmic fluorescence values were normalized against the average expression of reference genes *TOP1* and *EIF4A2*. Normalized data followed a Gaussian distribution and were used for statistical analysis.

For expression data, linear regression analyses were performed using IBM SPSS Statistics for Windows, Version 25.0 (IBM Corp., Armonk, NY) with normalized starting fluorescence values per isoform as dependent variable and diagnosis (control = 0, AD = 1, respectively), plaque load in the temporal lobe (0-3), tangle load in the temporal lobe (0-3), Braak stage level (Braak I-II = 0, Braak III-IV = 1, and Braak V-VI = 2), or MMSE score (0–30) as independent variable. Age, gender, PMI, *APOE* ε4 possession, and qPCR plate were included as covariates. Unstandardized regression coefficients were exponentially transformed to calculate the fold expression change in AD. *p* values were Bonferroni-corrected by multiplying *p* values by the number of dependent variables (i.e., expression of isoforms) tested per model, and values smaller than 0.05 were considered statistically significant.

For (hydroxy)methylomic data, a surrogate variable (SV) analysis was done with the sva package (version 3.30.1) (Leek et al., 2012) on an initial linear regression model with beta values as dependent variable, diagnosis as independent variable, and age, gender, PMI, and *APOE* ε4 possession as covariates. To adjust for unobserved confounders, the first 5 SVs of the SV analysis were included in the regression model. Linear regression was performed using the limma package (version 3.38.3) (Ritchie et al., 2015). Adjustment for bias and inflation of test statistics was done with the bacon package (version 1.10.1) (van Iterson et al., 2017). To explore whether isoform-specific expression changes could be mechanistically explained by specific epigenetic changes, only probes that locate closest to PDE4D isoform promoters showing significant expression changes (i.e., PDE4D1, -D3, -D5 and -D8) were selected (24 probes). Nominal significance for DNA methylation changes between AD cases and controls was set at p-value <0.05. Diagnosis-associated methylation changes were investigated further by follow-up linear regression analyses using the same model, but instead of diagnosis, using plaque load in the temporal lobe (0–3), tangle load

Table 3
PDE4D isoform expression in MTG tissue from AD patients compared to controls

Isoform expression	*N*	Diagnosis standardized coefficient	*p*-value Bonferroni-corrected	Fold change in AD
PDE4D1	82	0.383	0.013	2.99
PDE4D3	82	0.435	0.002	3.85
PDE4D4	67	0.259	0.487	2.14
PDE4D5	67	0.356	0.040	2.56
PDE4D6	77	0.267	0.257	2.90
PDE4D7	82	0.309	0.091	2.82
PDE4D8	62	0.394	0.045	3.85
PDE4D9	77	0.249	0.212	2.24

Linear regression analyses were performed according to the following formula: Expression = Intercept + Diagnosis + Gender + Age + *APOE* ε4 possession + PMI + qPCR plate. Significance levels are Bonferroni-corrected for the number of dependent variables tested. *p* values and fold changes are rounded to 3 and 2 decimals, respectively.
Key: AD, Alzheimer's disease; MTG, middle temporal gyrus; PDE4D, phosphodiesterase 4D; PMI, post-mortem interval; qPCR, quantitative polymerase chain reaction.

in the temporal lobe (0-3), Braak stage level (Braak I-II = 0, Braak III-IV = 1, and Braak V-VI = 2), or MMSE score (0–30) as predictor variable. False discovery rates for these predictors' *p* values were determined by the Benjamini-Hochberg procedure.

3. Results

3.1. Increased PDE4D isoform expression in Alzheimer's disease

Linear regression analyses revealed that AD diagnosis was significantly associated with increased expression levels of PDE4D1, -D3, -D5, and -D8, in the range of 2.56- to 3.85-fold increased expression ($p < 0.05$; Table 3).

3.2. Differential epigenetic signatures in PDE4D promoter regions in Alzheimer's disease

As *PDE4D* was found to be differentially methylated in AD in an epigenome-wide association study using the same tissue (Lardenoije et al., 2019), as an exploratory approach, we investigated whether 5'-cytosine-phosphate-guanine-3' sites within the promoter regions of differentially expressed PDE4D1, -D3, -D5, -D8 were subject to methylation differences. Twenty-four of the epigenome-wide association study assay probes located to these promoters and allowed the assessment of the methylation status (5mC, 5hmC, or UC) of specific 5'-cytosine-phosphate-guanine-3' sites. Linear regression analyses revealed diagnosis-dependent methylation status differences in each of the promoters. The 5'-cytosine-phosphate-guanine-3' sites for which methylation status was associated with diagnosis are shown in Table 4. AD-associated effects on methylation status appear to be different per promoter region. For example, in the PDE4D3 promoter, at position cg13112511, AD diagnosis was associated with decreased 5mC (fold change [FC] = 0.9818, $p < 0.05$) and increased 5hmC (FC = 1.0197, $p < 0.05$) levels. Contrastingly, increased 5mC (FC = 1.0144, $p < 0.01$) and decreased 5hmC (FC = 0.9812, $p < 0.05$) levels were found in the PDE4D8 promoter at cg23987137 in AD cases. Within the PDE4D5 promoter, effects with opposite directionality were found; increased 5mC and decreased UC levels were detected in AD cases at position cg03653541 (5mC: FC = 1.0023, $p < 0.05$ and UC: FC = 0.9972, $p < 0.05$), while position cg14784398 indicated decreased 5mC (FC = 0.9958, $p < 0.05$) and increased UC (FC = 1.0035, $p < 0.05$) levels. These findings suggest that AD is associated with *PDE4D* DNA (hydroxy)methylation changes that are promoter- and site-specific, concomitant with expression changes of the corresponding isoforms.

3.3. PDE4D isoform expression is associated with AD pathology and cognitive impairment

For isoforms showing different expression between AD and controls (i.e., PDE4D1, -D3, -D5, and -D8), linear regression analyses were performed to investigate whether expression was associated with the degree of pathology or cognitive impairment. Higher levels of plaque pathology in the temporal lobe were associated with increased PDE4D1 and -D3 expression ($p < 0.05$), while tangle pathology in the temporal lobe was associated with increased expression of PDE4D1 ($p < 0.05$), PDE4D3 ($p < 0.01$), and PDE4D5 ($p < 0.05$; Table 5 and Fig. 1). In addition, Braak staging associated significantly with increased expression of PDE4D1 ($p < 0.05$) and PDE4D3 ($p < 0.001$). Additionally, we examined the association between isoform expression and the level of cognitive impairment as assessed by the MMSE. Lower MMSE scores were significantly associated with increased expression of PDE4D1 ($p < 0.01$), PDE4D3 ($p < 0.01$), and PDE4D5 ($p < 0.05$; Table 5 and Fig. 1). These results indicate that increased expression, of mainly the PDE4D1 and PDE4D3 isoforms, correlates with higher pathology levels and more severe cognitive impairment.

3.4. PDE4D promoter methylation is associated with AD pathology and cognitive impairment

The diagnosis-dependent methylation changes as determined in Table 4 were investigated further for their potential association

Table 4
CpG sites in specific PDE4D promoter regions showing altered methylation status in AD

Promoter	*N*	CpG probe	Status	Fold change in AD	Mean	*t*	df	*p*-value
PDE4D1	78	cg19539826	UC	0.9871	0.5871	−2.363	67	0.018
PDE4D3	78	cg13112511	5mC	0.9818	0.3211	−2.571	67	0.010
	78	cg13112511	5hmC	1.0197	0.0537	2.299	67	0.022
PDE4D5	78	cg03653541	5mC	1.0023	0.0729	2.402	67	0.016
	78	cg14784398	5mC	0.9958	0.1267	−2.330	67	0.020
	78	cg12519013	5mC	0.9965	0.0849	−1.970	67	0.049
	78	cg14784398	UC	1.0035	0.8722	2.098	67	0.036
	78	cg03653541	UC	0.9972	0.9178	−2.010	67	0.044
PDE4D8	78	cg23987137	5mC	1.0144	0.3957	2.833	67	0.006
	78	cg23987137	5hmC	0.9812	0.1765	−2.391	67	0.017
	78	cg17584009	5hmC	1.0162	0.2300	1.961	67	0.050

Linear regressions were performed according to the following formula: Methylation status = Intercept + Diagnosis + Gender + Age + *APOE* ε4 possession + PMI + five surrogate variables.
Key: 5hmC, 5-hydroxymethylcytosine; 5mC, 5-methylcytosine; AD, Alzheimer's disease; df, degrees of freedom; PDE4D, phosphodiesterase 4D; PMI, post-mortem interval; UC, unmethylated cytosine.

Table 5
Association of pathology and cognitive impairment level with PDE4D isoform expression

Dependent variable		Standardized coefficient per pathology variable			Standardized coefficient for MMSE	
Isoform	*N*	Plaque load	Tangle load	Braak stage	*N*	MMSE
PDE4D1	82	0.313[a]	0.352[a]	0.445[a]	41	−0.577[b]
PDE4D3	82	0.332[a]	0.374[b]	0.508[c]	41	−0.610[b]
PDE4D5	67	0.207	0.344[a]	0.315	33	−0.475[a]
PDE4D8	62	0.211	0.203	0.178	32	−0.448

Linear regressions were performed according to the following formula: Expression = Intercept + Pathology variable (i.e., plaque load, tangle load, Braak) or MMSE + Gender + Age + *APOE* allele ε4 possession + PMI + qPCR plate. Cases for which MMSE scores were assessed more than 36 mo before death were excluded. Significance levels Bonferroni-corrected for the amount of dependent variables tested.
Key: MMSE, Mini-Mental State Examination; PDE4D, phosphodiesterase 4D; PMI, post-mortem interval; qPCR, quantitative polymerase chain reaction.
[a] $p < 0.05$.
[b] $p < 0.01$
[c] $p < 0.001$.

with the degree of pathology or cognitive impairment by means of linear regression analyses. These analyses revealed significant associations between methylation status changes and pathology or cognitive impairment in accordance to the directionality of changes observed between AD cases and controls. In the PDE4D3 promoter, both decreased 5mC (hypomethylation) and increased 5hmC (hyperhydroxymethylation) at CpG site cg13112511 were found to associate with an increased plaque load and a higher Braak stage (Table 6). Contrarily, in the PDE4D8 promoter, increased 5mC and decreased 5hmC at position cg23987137 was associated with increased pathology levels. Methylation status in the PDE4D5 promoter also associated with levels of pathology but the directionality of methylation status change was different per CpG site (e.g., cg03653541 shows increased 5mC, while cg12519013 shows decreased 5mC with higher levels of pathology; Table 6). Finally, lower MMSE scores were associated with increased 5mC levels in the PDE4D5 promoter (cg03653541) and PDE4D8 promoter (cg23987137).

4. Discussion

Inhibition of PDE4D has been shown to hold promise as an effective strategy to enhance memory in humans (clinical trials NCT02648672 and NCT02840279), but is also assumed to contribute to possible emetic side effects upon non-selective PDE4 inhibition (Giembycz, 2002; Mori et al., 2010). The *PDE4D* gene encodes multiple isoforms that, for example, by specific intracellular localization, can regulate different compartmentalized pools of cAMP (Houslay et al., 2007). Hence, targeting specific PDE4D isoforms may provide a safer and more efficacious treatment strategy to alleviate memory deficits in AD without evoking side effects (Schepers et al., 2019). To investigate which specific PDE4D isoform(s) is/are altered in terms of expression in AD, we established PDE4D isoform expression profiles in post-mortem MTG tissue derived from AD patients and healthy non-demented controls by means of isoform-specific qPCR.

Regression analyses revealed that AD was associated with increased expression of PDE4D1, -D3, -D5, and -D8. Expression of these isoforms was increased in the range of 2.56- to 3.85-fold. Previous studies have indicated that 3- to 4-fold increased PDE4D (isoform) mRNA expression results into similar increases in both PDE4D protein expression and PDE4 activity (Levallet et al., 2007; Peter et al., 2007). Therefore, the 2.59- to 3.85-fold expression increases likely increase PDE4 activity. To our knowledge, the number of studies investigating PDE4D expression in light of AD is limited. Ugarte et al. (2015) did not find a difference in overall PDE4D expression in temporal lobe material from AD patients ($n = 7$) and controls ($n = 8$). McLachlan et al. (2007) investigated hippocampal PDE4D isoform expression in material from a single patient with advanced AD and 3 control cases and found a 2.62-fold increase in PDE4D1 expression, while the expression of other isoforms was reduced or unaffected. Our study, making use of a much larger sample size, shows, in addition to a similar increase in PDE4D1 expression, increased expression of PDE4D3, -D5, and -D8. The current findings imply that PDE4D expression is affected in AD in an isoform-specific manner.

Because AD is a progressive disease, we also inspected whether PDE4D isoform expression increases with higher degrees of pathology or more severe cognitive impairment. Expression of PDE4D1 and PDE4D3 was associated with temporal plaque load, temporal tangle load, Braak staging, as well as cognitive impairment. PDE4D5 expression was found to be only associated with temporal tangle load and cognitive impairment, while PDE4D8 expression was not associated with any pathology measure or cognitive impairment. These findings suggest that mainly PDE4D1 and PDE4D3 expression changes as the disease progresses and cognitive impairment worsens. The observation that PDE4D3 transcription is increased in presence of higher amyloid-β plaque load corresponds to earlier findings. Hippocampal injections of $A\beta_{1-42}$ in mice caused memory deficits and increased protein expression of PDE4D3, which was reversed upon non-selective PDE4 inhibition by resveratrol (Wang et al., 2016). Interestingly, Olah et al., (2011) found a direct interaction between oligomeric Aβ and PDE4D. Whether this interaction occurs in vivo and how this interaction affects PDE4D enzymatic activity remains to be determined. From a potentially therapeutic perspective, it would be interesting to identify whether inhibition of PDE4D1 and/or PDE4D3 specifically can delay disease progression and improve cognitive functioning.

As the *PDE4D* gene, with its various isoforms embedded, contains multiple promoter regions, epigenetic mechanisms are likely involved in its isoform-specific expression regulation, for example, by influencing promoter accessibility (Maunakea et al., 2010; Tilley and Maurice, 2005). Here, we found that DNA (hydroxy)methylation signatures in the promoter regions of PDE4D1, -D3, -D5, and -D8 were altered in the same tissue as used for the expression profiling. Results showed differentially methylated CpG sites in these promoters that were associated with AD diagnosis. Moreover, methylation status was also associated with the degree of pathology and cognitive impairment for several CpG sites. Various effects were observed, that is, both increased and decreased 5mC, 5hmC, and UC levels. Differences in methylation and hydroxymethylation can be linked to altered gene expression by affecting the binding of transcription factors and chromatin proteins to the DNA (Suzuki and Bird, 2008; Yin et al., 2017). As such, decreased methylation and increased hydroxymethylation in AD in the PDE4D3 promoter might explain, at least in part, the observed pathology- and AD-associated increased expression of PDE4D3. In contrast, in the PDE4D8 promoter, cg23987137 displayed AD-associated hypermethylation and hypohydroxymethylation. However, cytosine methylation can have differential effects on transcription factor binding and subsequent gene expression. Interestingly, cg23987137 is located 14 nucleotides downstream of an activator protein 1 (AP-1) binding site (Farre et al., 2003). The transcription factor AP-1 is usually described as a transcriptional activator, but can also act as transcriptional repressor (Brellier et al., 2004). Moreover, it has been shown that methylation adjacent to, but not within, the AP-1 binding site can hamper AP-1 binding and consequently induce transcription (Fujimoto et al., 2005). Although purely speculative, a

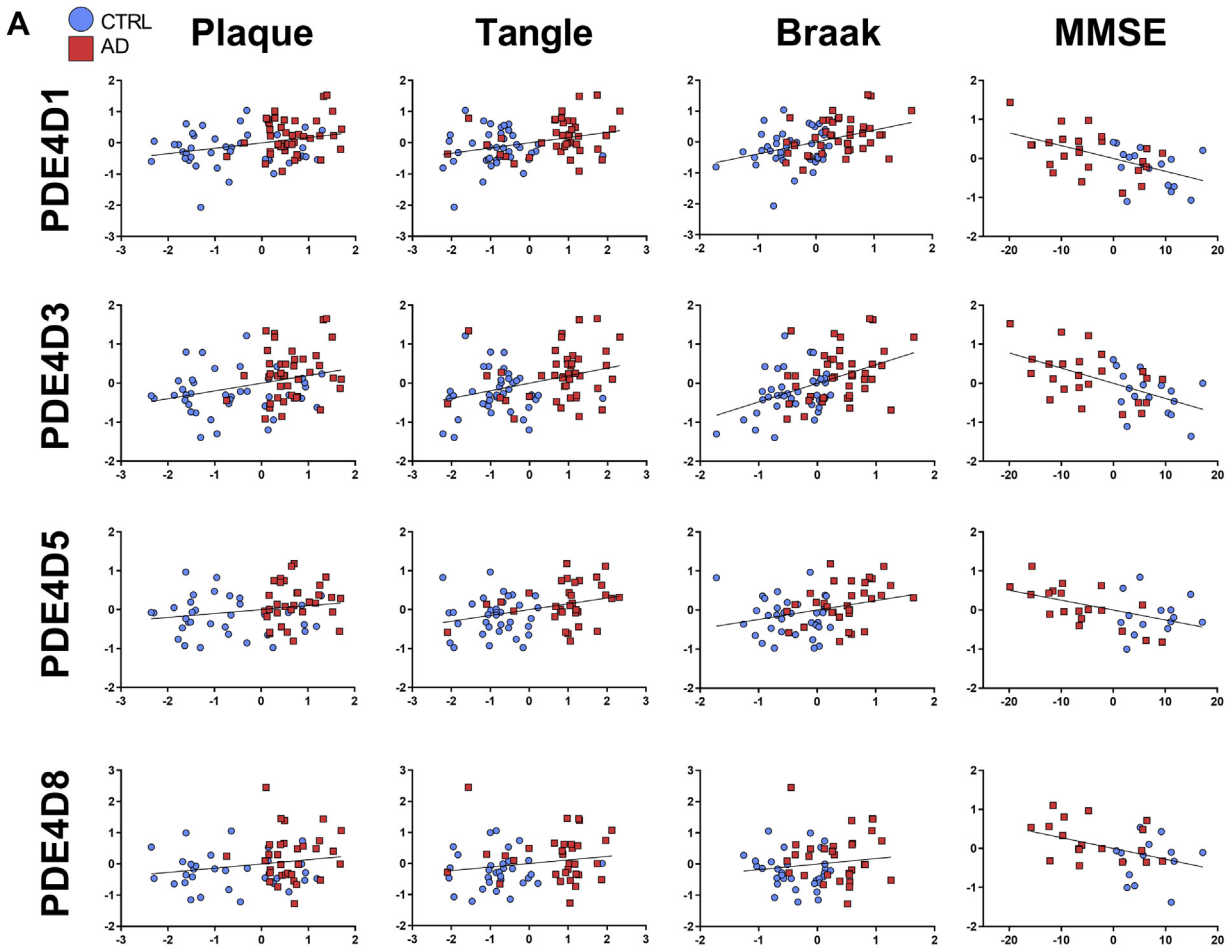

B

	Plaque		Tangle		Braak		MMSE	
	β	R^2	β	R^2	β	R^2	β	R^2
D1	0.173*	0.09	0.168*	0.11	0.385*	0.17	-0.033**	0.30
D3	0.199*	0.10	0.194**	0.13	0.476***	0.22	-0.039**	0.32
D5	0.100	0.04	0.151*	0.12	0.242	0.10	-0.026*	0.24
D8	0.138	0.04	0.117	0.03	0.186	0.02	-0.030	0.17

Fig. 1. Association of pathology and cognitive impairment level with PDE4D isoform expression. (A) Partial regression plots visualizing the associations between PDE4D isoform expression and the degree of pathology (plaque and tangle load in the temporal lobe, and Braak stage level) or cognitive impairment (MMSE score), corrected for gender, age, APOE allele ε4 possession, PMI, and qPCR plate. Marker types reflect the diagnosis status of the cases (blue circles: controls, red squares: AD cases). (B) Overview of slope values (β) and squared correlation coefficients of the regression lines in the partial regression plots in panel A. β values correspond to the unstandardized coefficients of pathology and MMSE variables in the regressions according to the formula described in Table 5. Significance levels Bonferroni-corrected for the amount of dependent variables tested; $^{*}p < 0.05$, $^{**}p < 0.01$, $^{***}p < 0.001$. Abbreviations: AD, Alzheimer's disease; CTRL, control; MMSE, Mini-Mental State Examination; PDE4D, phosphodiesterase 4D; PMI, post-mortem interval; qPCR, quantitative polymerase chain reaction. (For interpretation of the references to color in this figure legend, the reader is referred to the Web version of this article.)

similar mechanism might affect transcription near the PDE4D8 promoter resulting in increased expression upon CpG site hypermethylation. Similarly, epigenetic changes observed in the other promoters can, by influencing binding of transcriptional activators and repressors, induce increased expression of the associated isoforms. Interestingly, increased methylation at cg23987137 PDE4D8 promoter was associated with worse cognitive performance while PDE4D8 expression did not associate with cognitive performance. This discrepancy may suggest that DNA methylation may not solely influence expression via its closest located promoter but may also regulate expression of other isoforms which do show associations with cognitive performance (i.e., PDE4D1, -D3, and -D5).

The current findings show that in AD, expression of specific PDE4D isoforms is altered with concurrent changes (hydroxy) methylation changes in associated promoters of the *PDE4D* gene. Although PDE4D isoforms locate to specific cellular compartments, the role of individual PDE4D isoforms in specific cellular processes is still largely unknown. The mouse orthologue of PDE4D1 is reported to localize to the nucleus (Chandrasekaran et al., 2008). With 95.6% homology in the N-terminal, human PDE4D1 may share a similar localization signal and hence could be involved in the regulation of nuclear cAMP levels which may directly affect PKA-CREB mediated transcription crucial for memory consolidation (Kandel, 2012). Transgenic overexpression of PDE4D1 in specific

Table 6
Significant associations of PDE4D promoter methylation status with pathology and cognitive impairment

Promoter	CpG probe	Status	*N*	Variable	Fold change	Mean	*t*	df	*p*-value	FDR
PDE4D3	cg13112511	5mC	78	Plaque	0.9917	0.3211	−2.561	67	0.010	0.017
			78	Braak	0.9858	0.3211	−2.929	67	0.003	0.008
		5hmC	78	Plaque	1.0095	0.0537	2.456	67	0.014	0.042
			78	Braak	1.0167	0.0537	2.674	67	0.007	0.011
PDE4D5	cg03653541	5mC	78	Tangle	1.0010	0.0729	2.805	67	0.005	0.025
			78	Braak	1.0014	0.0729	2.104	67	0.035	0.035
			39	MMSE	0.9997	0.0732	−3.533	28	<0.001	0.001
		UC	78	Plaque	0.9984	0.9178	−2.533	67	0.011	0.034
	cg14784398	5mC	78	Tangle	0.9983	0.1267	−2.363	67	0.018	0.030
			78	Braak	0.9972	0.1267	−2.200	67	0.028	0.035
		UC	78	Plaque	1.0015	0.8722	2.175	67	0.030	0.044
	cg12519013	5mC	78	Plaque	0.9980	0.0849	−2.612	67	0.009	0.022
			78	Tangle	0.9985	0.0849	−2.157	67	0.031	0.039
			78	Braak	0.9973	0.0849	−2.202	67	0.027	0.046
PDE4D8	cg23987137	5mC	78	Plaque	1.0063	0.3957	2.791	67	0.005	0.026
			78	Tangle	1.0047	0.3957	2.384	67	0.017	0.043
			78	Braak	1.0108	0.3957	3.034	67	0.002	0.012
			39	MMSE	0.9987	0.4035	−4.126	28	<0.001	<0.001
		5hmC	78	Plaque	0.9922	0.1765	−2.178	67	0.029	0.044
			78	Braak	0.9851	0.1765	−2.735	67	0.006	0.019

Linear regressions were performed according to the following formula: Methylation status = Intercept + Pathology variable (i.e., plaque load, tangle load, Braak) or MMSE + Gender + Age + *APOE ε4* possession + PMI + five surrogate variables. Cases for which MMSE scores were assessed more than 36 mo before death were excluded.
Key: 5hmC, 5-hydroxymethylcytosine; 5mC, 5-methylcytosine; df, degrees of freedom; FDR, false discovery rate (Benjamini-Hochberg); MMSE, Mini-Mental State Examination; PDE4D, phosphodiesterase 4D; UC, unmethylated cytosine.

neurons was found to decrease Ca^{2+} oscillations, which may imply a specific role for this isoform in neuronal firing (Yoshida et al., 2003). Increased PDE4D1 expression in AD may therefore decrease neuronal firing rates that subsequently impacts neuronal plasticity and memory formation processes.

Specific interactions have been reported between PDE4D3 and A-kinase anchoring proteins (AKAPs), for example, AKAP9 and mAKAPα, through which PDE4D3 can locally degrade cAMP pools (Boczek et al., 2019; Terrenoire et al., 2009). Disrupting the perinuclear PDE4D3-mAKAPα signaling complex promoted survival and axon growth in neurons (Boczek et al., 2019). Vice versa, increased PDE4D3 expression as observed in the current study could hamper these effects, thereby likely impairing neuronal plasticity and memory processes in AD.

Similar to PDE4D3-AKAP interactions, the scaffolding protein β-arrestin was found to preferentially interact with PDE4D5 (Baillie et al., 2007). β-arrestin is recruited to G-protein coupled receptors (GPCRs) upon activation, which places PDE4D5 in close proximity to sites where cAMP is produced, that is, close to GPCRs and activated adenylyl cyclases that produce cAMP (Baillie et al., 2003; Houslay and Baillie, 2005). Increased PDE4D5 levels may therefore excessively degrade cAMP at the site of synthesis. Vice versa, downregulation of PDE4D5 may stimulate cAMP signaling, which is supported by the interesting finding that knockdown of PDE4D4 or PDE4D5 can improve memory performance in mice (MacKenzie et al., 2011; Wang et al., 2013). In addition to cytosolic interactions, it was found that PDE4D5 also regulates cAMP levels in nuclear signaling complexes, indicating that a specific isoform can regulate cAMP levels in spatially distinct compartments (Clister et al., 2019).

Regarding PDE4D8, most insights have been gathered through cardiovascular research. In cardiomyocytes, PDE4D8 is located near the β1-adrenergic receptor through a SAP97-mediated interaction and dissociates upon receptor stimulation (Fu et al., 2014; Richter et al., 2008). As SAP97 is a synapse-associated protein that scaffolds multiple receptors, including AMPA receptors crucial for memory processes, similar interactions may occur in the brain (Zhang et al., 2015). Moreover, PDE4D8 is found to localize in leading-edge structures of migrating vascular smooth muscle cells and affects actin organization upon overexpression (Raymond et al., 2009). Actin-rich leading edges in neuronal or glial cells may also be affected by increased PDE4D8 levels and consequently induce dysfunctional migration and growth, possibly contributing to impaired cognitive functioning eventually.

Through their specific localizations, the isoforms PDE4D3, -D5, and -D8 have all been reported to modulate downstream signaling of β-adrenergic receptors (Baillie et al., 2003; De Arcangelis et al., 2009; Richter et al., 2008). As adrenergic signaling is involved in cognitive functioning and can be affected in AD (Gannon et al., 2015), changes in expression of PDE4D isoforms may disrupt downstream β-adrenergic signaling leading to cognitive dysfunction. In sum, upcoming studies will have to indicate isoform-specific roles in memory processes, so local cAMP compartments can be targeted and treatment efficacy can be increased.

Finally, the current findings represent PDE4D isoform expression and DNA (hydroxy)methylation in homogenized brain tissue, meaning no conclusions can be drawn yet on potential cell type-specific effects. Hence, follow-up studies will have to indicate whether the current findings can be linked to changes in specific cell types (e.g., neurons, microglia, astrocytes, oligodendrocytes, endothelial cells). Also, whether increased PDE4D expression is causal to or a consequence of worsening pathology remains to be specified. Nevertheless, these findings highlight isoform-specific PDE4D inhibition as a potential strategy to aid in delaying disease progression with associated procognitive effects.

5. Conclusions

Taken together, regulation of PDE4D transcription is affected in AD as indicated by differences in gene (hydroxy)methylation and expression levels. Moreover, the specific isoforms PDE4D1 and PDE4D3 show a significant association with the degree of pathology and cognitive impairment. In line with the fact that PDE4D isoforms regulate specific intracellular processes, this implies that targeting specific PDE4D isoforms may provide a more efficacious treatment strategy with less adverse effects in different stages of the disease. For this purpose, future studies will have to reveal which PDE4D isoforms regulate mechanisms underlying memory enhancement and do not show adverse effects upon inhibition in the context of brain function in both health and AD.

Disclosure statement

Vanmierlo and Prickaerts have a proprietary interest in selective PDE4D inhibitors for the treatment of neurodegenerative disorders. The other authors declare that they have no competing interests.

CRediT authorship contribution statement

Dean Paes: Investigation, Formal analysis, Writing - original draft. **Roy Lardenoije:** Investigation, Formal analysis, Writing - review & editing. **Riccardo M. Carollo:** Formal analysis, Writing - review & editing. **Janou A.Y. Roubroeks:** Formal analysis, Writing - review & editing. **Melissa Schepers:** Formal analysis, Writing - review & editing. **Paul Coleman:** Resources. **Diego Mastroeni:** Resources. **Elaine Delvaux:** Resources. **Ehsan Pishva:** Formal analysis, Writing - review & editing. **Katie Lunnon:** Formal analysis, Writing - review & editing. **Tim Vanmierlo:** Conceptualization, Writing - review & editing, Supervision, Project administration, Funding acquisition. **Daniel van den Hove:** Conceptualization, Writing - review & editing, Supervision, Project administration, Funding acquisition. **Jos Prickaerts:** Conceptualization, Writing - review & editing, Supervision, Project administration, Funding acquisition.

Acknowledgements

This work was financially supported by grants from ISAO/Alzheimer Nederland WE.03-2016-07, Young European Research Universities Network (YERUN), and the Baeter Laeve foundation. Additional funds have been provided by the Internationale Stichting Alzheimer Onderzoek (ISAO)/Alzheimer Netherlands (Award #11532; Funded by the Dorpmans-Wigmans Foundation) (DvdH), and by the Joint Programme—Neurodegenerative Disease Research (JPND) for the EPI-AD consortium (http://www.neurodegenerationresearch.eu/wp-content/uploads/2015/10/Factsheet_EPI-AD.pdf). The project is supported through the following funding organizations under the aegis of JPND; The Netherlands, The Netherlands Organisation for Health Research and Development (ZonMw); United Kingdom, Medical Research Council; Germany, German Federal Ministry of Education and Research (BMBF); Luxembourg, National Research Fund (FNR). This project has received funding from the European Union's Horizon 2020 research and innovation program under Grant Agreement No. 643417.

We thank Dr. Ir. Jochen De Vry for primer and qPCR experiment design.

References

Aryee, M.J., Jaffe, A.E., Corrada-Bravo, H., Ladd-Acosta, C., Feinberg, A.P., Hansen, K.D., Irizarry, R.A., 2014. Minfi: a flexible and comprehensive Bioconductor package for the analysis of Infinium DNA methylation microarrays. Bioinformatics (Oxford, England) 30, 1363–1369.

Baillie, G.S., Adams, D.R., Bhari, N., Houslay, T.M., Vadrevu, S., Meng, D., Li, X., Dunlop, A., Milligan, G., Bolger, G.B., Klussmann, E., Houslay, M.D., 2007. Mapping binding sites for the PDE4D5 cAMP-specific phosphodiesterase to the N- and C-domains of beta-arrestin using spot-immobilized peptide arrays. Biochem. J. 404, 71–80.

Baillie, G.S., Sood, A., McPhee, I., Gall, I., Perry, S.J., Lefkowitz, R.J., Houslay, M.D., 2003. beta-Arrestin-mediated PDE4 cAMP phosphodiesterase recruitment regulates beta-adrenoceptor switching from Gs to Gi. Proc. Natl. Acad. Sci. U. S. A. 100, 940–945.

Baumgartel, K., Green, A., Hornberger, D., Lapira, J., Rex, C., Wheeler, D.G., Peters, M., 2018. PDE4D regulates spine plasticity and memory in the retrosplenial cortex. Sci. Rep. 8, 3895.

Beach, T.G., Adler, C.H., Sue, L.I., Serrano, G., Shill, H.A., Walker, D.G., Lue, L., Roher, A.E., Dugger, B.N., Maarouf, C., Birdsill, A.C., Intorcia, A., Saxon-Labelle, M., Pullen, J., Scroggins, A., Filon, J., Scott, S., Hoffman, B., Garcia, A., Caviness, J.N., Hentz, J.G., Driver-Dunckley, E., Jacobson, S.A., Davis, K.J., Belden, C.M., Long, K.E., Malek-Ahmadi, M., Powell, J.J., Gale, L.D., Nicholson, L.R., Caselli, R.J., Woodruff, B.K., Rapscak, S.Z., Ahern, G.L., Shi, J., Burke, A.D., Reiman, E.M., Sabbagh, M.N., 2015. Arizona Study of Aging and Neurodegenerative disorders and brain and body donation program. Neuropathology 35, 354–389.

Blokland, A., Van Duinen, M.A., Sambeth, A., Heckman, P.R.A., Tsai, M., Lahu, G., Uz, T., Prickaerts, J., 2019. Acute treatment with the PDE4 inhibitor roflumilast improves verbal word memory in healthy old individuals: a double-blind placebo-controlled study. Neurobiol. Aging 77, 37–43.

Boczek, T., Cameron, E.G., Yu, W., Xia, X., Shah, S.H., Castillo Chabeco, B., Galvao, J., Nahmou, M., Li, J., Thakur, H., Goldberg, J.L., Kapiloff, M.S., 2019. Regulation of neuronal survival and axon growth by a perinuclear cAMP compartment. J. Neurosci. 39, 5466–5480.

Braak, H., Braak, E., 1991. Demonstration of amyloid deposits and neurofibrillary changes in whole brain sections. Brain Pathol. 1, 213–216.

Brellier, F., Marionnet, C., Chevallier-Lagente, O., Toftgard, R., Mauviel, A., Sarasin, A., Magnaldo, T., 2004. Ultraviolet irradiation represses PATCHED gene transcription in human epidermal keratinocytes through an activator protein-1-dependent process. Cancer Res. 64, 2699–2704.

Chandrasekaran, A., Toh, K.Y., Low, S.H., Tay, S.K., Brenner, S., Goh, D.L., 2008. Identification and characterization of novel mouse PDE4D isoforms: molecular cloning, subcellular distribution and detection of isoform-specific intracellular localization signals. Cell Signal 20, 139–153.

Chen, Y.A., Lemire, M., Choufani, S., Butcher, D.T., Grafodatskaya, D., Zanke, B.W., Gallinger, S., Hudson, T.J., Weksberg, R., 2013. Discovery of cross-reactive probes and polymorphic CpGs in the Illumina Infinium HumanMethylation450 microarray. Epigenetics 8, 203–209.

Cheng, Y.F., Wang, C., Lin, H.B., Li, Y.F., Huang, Y., Xu, J.P., Zhang, H.T., 2010. Inhibition of phosphodiesterase-4 reverses memory deficits produced by Abeta25-35 or Abeta1-40 peptide in rats. Psychopharmacology 212, 181–191.

Clister, T., Greenwald, E.C., Baillie, G.S., Zhang, J., 2019. AKAP95 organizes a nuclear microdomain to control local cAMP for regulating nuclear PKA. Cell Chem. Biol. 26, 885–891.

Consensus Recommendations for the Postmortem Diagnosis of Alzheimer's Disease, 1997. The National Institute on Aging, and Reagan Institute Working Group on Diagnostic Criteria for the Neuropathological Assessment of Alzheimer's Disease. Neurobiol. Aging 18 (4 Suppl), S1–S2.

De Arcangelis, V., Liu, R., Soto, D., Xiang, Y., 2009. Differential association of phosphodiesterase 4D isoforms with beta2-adrenoceptor in cardiac myocytes. J. Biol. Chem. 284, 33824–33832.

Farre, D., Roset, R., Huerta, M., Adsuara, J.E., Rosello, L., Alba, M.M., Messeguer, X., 2003. Identification of patterns in biological sequences at the ALGGEN server: PROMO and MALGEN. Nucleic Acids Res. 31, 3651–3653.

Folstein, M.F., Folstein, S.E., McHugh, P.R., 1975. Mini-mental state". A practical method for grading the cognitive state of patients for the clinician. J. Psychiatr. Res. 12, 189–198.

Fu, Q., Kim, S., Soto, D., De Arcangelis, V., DiPilato, L., Liu, S., Xu, B., Shi, Q., Zhang, J., Xiang, Y.K., 2014. A long lasting beta1 adrenergic receptor stimulation of cAMP/protein kinase A (PKA) signal in cardiac myocytes. J. Biol. Chem. 289, 14771–14781.

Fujimoto, M., Kitazawa, R., Maeda, S., Kitazawa, S., 2005. Methylation adjacent to negatively regulating AP-1 site reactivates TrkA gene expression during cancer progression. Oncogene 24, 5108–5118.

Gannon, M., Che, P., Chen, Y., Jiao, K., Roberson, E.D., Wang, Q., 2015. Noradrenergic dysfunction in Alzheimer's disease. Front Neurosci. 9, 220, 220.

Giembycz, M.A., 2002. 4D or not 4D - the emetogenic basis of PDE4 inhibitors uncovered? Trends Pharmacol. Sci. 23, 548.

Houslay, M.D., 2010. Underpinning compartmentalised cAMP signalling through targeted cAMP breakdown. Trends Biochem. Sci. 35, 91–100.

Houslay, M.D., Baillie, G.S., 2005. Beta-arrestin-recruited phosphodiesterase-4 desensitizes the AKAP79/PKA-mediated switching of beta2-adrenoceptor signalling to activation of ERK. Biochem. Soc. Trans. 33 (Pt 6), 1333–1336.

Houslay, M.D., Baillie, G.S., Maurice, D.H., 2007. cAMP-specific phosphodiesterase-4 enzymes in the cardiovascular system: a molecular toolbox for generating compartmentalized cAMP signaling. Circ. Res. 100, 950–966.

Kandel, E.R., 2012. The molecular biology of memory: cAMP, PKA, CRE, CREB-1, CREB-2, and CPEB. Mol. Brain 5, 14.

Kiihl, S.F., Martinez-Garrido, M.J., Domingo-Relloso, A., Bermudez, J., Tellez-Plaza, M., 2019. MLML2R: an R package for maximum likelihood estimation of DNA methylation and hydroxymethylation proportions. Stat. Appl. Genet. Mol. Biol. 18.

Lardenoije, R., Roubroeks, J.A.Y., Pishva, E., Leber, M., Wagner, H., Iatrou, A., Smith, A.R., Smith, R.G., Eijssen, L.M.T., Kleineidam, L., Kawalia, A., Hoffmann, P., Luck, T., Riedel-Heller, S., Jessen, F., Maier, W., Wagner, M., Hurlemann, R., Kenis, G., Ali, M., Del Sol, A., Mastroeni, D., Delvaux, E., Coleman, P.D., Mill, J., Rutten, B.P.F., Lunnon, K., Ramirez, A., van den Hove, D.L.A., 2019. Alzheimer's disease-associated (hydroxy)methylomic changes in the brain and blood. Clin. Epigenetics 11, 164.

Leek, J.T., Johnson, W.E., Parker, H.S., Jaffe, A.E., Storey, J.D., 2012. The sva package for removing batch effects and other unwanted variation in high-throughput experiments. Bioinformatics (Oxford, England) 28, 882–883.

Levallet, G., Levallet, J., Bouraima-Lelong, H., Bonnamy, P.J., 2007. Expression of the cAMP-phosphodiesterase PDE4D isoforms and age-related changes in follicle-stimulating hormone-stimulated PDE4 activities in immature rat Sertoli cells. Biol. Reprod. 76, 794–803.

MacKenzie, K.F., Wallace, D.A., Hill, E.V., Anthony, D.F., Henderson, D.J., Houslay, D.M., Arthur, J.S., Baillie, G.S., Houslay, M.D., 2011. Phosphorylation of cAMP-specific PDE4A5 (phosphodiesterase-4A5) by MK2 (MAPKAPK2)

attenuates its activation through protein kinase A phosphorylation. Biochem. J. 435, 755–769.
Maunakea, A.K., Nagarajan, R.P., Bilenky, M., Ballinger, T.J., D'Souza, C., Fouse, S.D., Johnson, B.E., Hong, C., Nielsen, C., Zhao, Y., Turecki, G., Delaney, A., Varhol, R., Thiessen, N., Shchors, K., Heine, V.M., Rowitch, D.H., Xing, X., Fiore, C., Schillebeeckx, M., Jones, S.J., Haussler, D., Marra, M.A., Hirst, M., Wang, T., Costello, J.F., 2010. Conserved role of intragenic DNA methylation in regulating alternative promoters. Nature 466, 253–257.
McLachlan, C.S., Chen, M.L., Lynex, C.N., Goh, D.L., Brenner, S., Tay, S.K., 2007. Changes in PDE4D isoforms in the hippocampus of a patient with advanced Alzheimer disease. Arch. Neurol. 64, 456–457.
Mori, F., Perez-Torres, S., De Caro, R., Porzionato, A., Macchi, V., Beleta, J., Gavalda, A., Palacios, J.M., Mengod, G., 2010. The human area postrema and other nuclei related to the emetic reflex express cAMP phosphodiesterases 4B and 4D. J. Chem. Neuroanat. 40, 36–42.
Myeku, N., Clelland, C.L., Emrani, S., Kukushkin, N.V., Yu, W.H., Goldberg, A.L., Duff, K.E., 2016. Tau-driven 26S proteasome impairment and cognitive dysfunction can be prevented early in disease by activating cAMP-PKA signaling. Nat. Med. 22, 46–53.
Olah, J., Vincze, O., Virok, D., Simon, D., Bozso, Z., Tokesi, N., Horvath, I., Hlavanda, E., Kovacs, J., Magyar, A., Szucs, M., Orosz, F., Penke, B., Ovadi, J., 2011. Interactions of pathological hallmark proteins: tubulin polymerization promoting protein/p25, beta-amyloid, and alpha-synuclein. J. Biol. Chem. 286, 34088–34100.
Perez-Torres, S., Miro, X., Palacios, J.M., Cortes, R., Puigdomenech, P., Mengod, G., 2000. Phosphodiesterase type 4 isozymes expression in human brain examined by in situ hybridization histochemistry and[3H]rolipram binding autoradiography. Comparison with monkey and rat brain. J. Chem. Neuroanat. 20, 349–374.
Peter, D., Jin, S.L., Conti, M., Hatzelmann, A., Zitt, C., 2007. Differential expression and function of phosphodiesterase 4 (PDE4) subtypes in human primary CD4+ T cells: predominant role of PDE4D. J. Immunol. 178, 4820–4831.
Pidsley, R., CC, Y.W., Volta, M., Lunnon, K., Mill, J., Schalkwyk, L.C., 2013. A data-driven approach to preprocessing Illumina 450K methylation array data. BMC Genomics 14, 293.
Qu, J., Zhou, M., Song, Q., Hong, E.E., Smith, A.D., 2013. MLML: consistent simultaneous estimates of DNA methylation and hydroxymethylation. Bioinformatics (Oxford, England) 29, 2645–2646.
R Development Core Team, 2019. R: A Language and Environment for Statistical Computing. R Foundation for Statistical Computing, Vienna, Austria. https://www.r-project.org/. (Accessed 16 September 2019).
Raymond, D.R., Carter, R.L., Ward, C.A., Maurice, D.H., 2009. Distinct phosphodiesterase-4D variants integrate into protein kinase A-based signaling complexes in cardiac and vascular myocytes. Am. J. Physiol. Heart Circ. Physiol. 296, H263–H271.
Ricciarelli, R., Brullo, C., Prickaerts, J., Arancio, O., Villa, C., Rebosio, C., Calcagno, E., Balbi, M., van Hagen, B.T., Argyrousi, E.K., Zhang, H., Pronzato, M.A., Bruno, O., Fedele, E., 2017. Memory-enhancing effects of GEBR-32a, a new PDE4D inhibitor holding promise for the treatment of Alzheimer's disease. Sci. Rep. 7, 46320.
Richter, W., Day, P., Agrawal, R., Bruss, M.D., Granier, S., Wang, Y.L., Rasmussen, S.G., Horner, K., Wang, P., Lei, T., Patterson, A.J., Kobilka, B., Conti, M., 2008. Signaling from beta1- and beta2-adrenergic receptors is defined by differential interactions with PDE4. EMBO J. 27, 384–393.
Ritchie, M.E., Phipson, B., Wu, D., Hu, Y., Law, C.W., Shi, W., Smyth, G.K., 2015. Limma powers differential expression analyses for RNA-sequencing and microarray studies. Nucleic Acids Res. 43, e47.
Robichaud, A., Stamatiou, P.B., Jin, S.L., Lachance, N., MacDonald, D., Laliberte, F., Liu, S., Huang, Z., Conti, M., Chan, C.C., 2002. Deletion of phosphodiesterase 4D in mice shortens alpha(2)-adrenoceptor-mediated anesthesia, a behavioral correlate of emesis. J. Clin. Invest. 110, 1045–1052.
RStudio Team, 2019. RStudio: Integrated Development for R RStudio, Inc., Boston, MA. htttp://www.rstudio.com/. (Accessed 16 September 2019).
Ruijter, J.M., Ramakers, C., Hoogaars, W.M., Karlen, Y., Bakker, O., van den Hoff, M.J., Moorman, A.F., 2009. Amplification efficiency: linking baseline and bias in the analysis of quantitative PCR data. Nucleic Acids Res. 37, e45.
Schepers, M., Tiane, A., Paes, D., Sanchez, S., Rombaut, B., Piccart, E., Rutten, B.P.F., Brône, B., Hellings, N., Prickaerts, J., Vanmierlo, T., 2019. Targeting phosphodiesterases—towards a tailor-made approach in multiple sclerosis treatment. Front. Immunol. 10.
Schneider, J., Murray, J., Banerjee, S., Mann, A., 1999. EUROCARE: a cross-national study of co-resident spouse carers for people with Alzheimer's disease: I—factors associated with carer burden. Int. J. Geriatr. Psychiatry 14, 651–661.
Smith, A.R., Smith, R.G., Pishva, E., Hannon, E., Roubroeks, J.A.Y., Burrage, J., Troakes, C., Al-Sarraj, S., Sloan, C., Mill, J., van den Hove, D.L., Lunnon, K., 2019. Parallel profiling of DNA methylation and hydroxymethylation highlights neuropathology-associated epigenetic variation in Alzheimer's disease. Clin. Epigenetics 11, 52.
Suzuki, M.M., Bird, A., 2008. DNA methylation landscapes: provocative insights from epigenomics. Nat. Rev. Genet. 9, 465–476.
Terrenoire, C., Houslay, M.D., Baillie, G.S., Kass, R.S., 2009. The cardiac IKs potassium channel macromolecular complex includes the phosphodiesterase PDE4D3. J. Biol. Chem. 284, 9140–9146.
Tilley, D.G., Maurice, D.H., 2005. Vascular smooth muscle cell phenotype-dependent phosphodiesterase 4D short form expression: role of differential histone acetylation on cAMP-regulated function. Mol. Pharmacol. 68, 596–605.
Ugarte, A., Gil-Bea, F., Garcia-Barroso, C., Cedazo-Minguez, A., Ramirez, M.J., Franco, R., Garcia-Osta, A., Oyarzabal, J., Cuadrado-Tejedor, M., 2015. Decreased levels of guanosine 3', 5'-monophosphate (cGMP) in cerebrospinal fluid (CSF) are associated with cognitive decline and amyloid pathology in Alzheimer's disease. Neuropathol. Appl. Neurobiol. 41, 471–482.
Van Duinen, M.A., Sambeth, A., Heckman, P.R.A., Smit, S., Tsai, M., Lahu, G., Uz, T., Blokland, A., Prickaerts, J., 2018. Acute administration of roflumilast enhances immediate recall of verbal word memory in healthy young adults. Neuropharmacology 131, 31–38.
van Iterson, M., van Zwet, E.W., Consortium, B., Heijmans, B.T., 2017. Controlling bias and inflation in epigenome- and transcriptome-wide association studies using the empirical null distribution. Genome Biol. 18, 19.
Vandesompele, J., De Preter, K., Pattyn, F., Poppe, B., Van Roy, N., De Paepe, A., Speleman, F., 2002. Accurate normalization of real-time quantitative RT-PCR data by geometric averaging of multiple internal control genes. Genome Biol. 3.
Vanmierlo, T., Creemers, P., Akkerman, S., van Duinen, M., Sambeth, A., De Vry, J., Uz, T., Blokland, A., Prickaerts, J., 2016. The PDE4 inhibitor roflumilast improves memory in rodents at non-emetic doses. Behav. Brain Res. 303, 26–33.
Wang, G., Chen, L., Pan, X., Chen, J., Wang, L., Wang, W., Cheng, R., Wu, F., Feng, X., Yu, Y., Zhang, H.T., O'Donnell, J.M., Xu, Y., 2016. The effect of resveratrol on beta amyloid-induced memory impairment involves inhibition of phosphodiesterase-4 related signaling. Oncotarget 7, 17380–17392.
Wang, Z.Z., Zhang, Y., Liu, Y.Q., Zhao, N., Zhang, Y.Z., Yuan, L., An, L., Li, J., Wang, X.Y., Qin, J.J., Wilson, S.P., O'Donnell, J.M., Zhang, H.T., Li, Y.F., 2013. RNA interference-mediated phosphodiesterase 4D splice variants knock-down in the prefrontal cortex produces antidepressant-like and cognition-enhancing effects. Br. J. Pharmacol. 168, 1001–1014.
Yin, Y., Morgunova, E., Jolma, A., Kaasinen, E., Sahu, B., Khund-Sayeed, S., Das, P.K., Kivioja, T., Dave, K., Zhong, F., Nitta, K.R., Taipale, M., Popov, A., Ginno, P.A., Domcke, S., Yan, J., Schubeler, D., Vinson, C., Taipale, J., 2017. Impact of cytosine methylation on DNA binding specificities of human transcription factors. Science 356.
Yoshida, H., Beltran-Parrazal, L., Butler, P., Conti, M., Charles, A.C., Weiner, R.I., 2003. Lowering cyclic adenosine-3',5'-monophosphate (cAMP) levels by expression of a cAMP-specific phosphodiesterase decreases intrinsic pulsatile gonadotropin-releasing hormone secretion from GT1 cells. Mol. Endocrinol. 17, 1982–1990.
Zhang, L., Hsu, F.C., Mojsilovic-Petrovic, J., Jablonski, A.M., Zhai, J., Coulter, D.A., Kalb, R.G., 2015. Structure-function analysis of SAP97, a modular scaffolding protein that drives dendrite growth. Mol. Cell Neurosci. 65, 31–44.
Zhang, C., Xu, Y., Chowdhary, A., Fox 3rd, D., Gurney, M.E., Zhang, H.T., Auerbach, B.D., Salvi, R.J., Yang, M., Li, G., O'Donnell, J.M., 2018. Memory enhancing effects of BPN14770, an allosteric inhibitor of phosphodiesterase-4D, in wild-type and humanized mice. Neuropsychopharmacology 43, 2299–2309.
Zhang, C., Xu, Y., Zhang, H.T., Gurney, M.E., O'Donnell, J.M., 2017. Comparison of the pharmacological profiles of selective PDE4B and PDE4D inhibitors in the central nervous system. Sci. Rep. 7, 40115.